Clinical and Experimental Dermatology and Therapies

OPEN ACCESS

Veraldi S, et al. Clin Exp Dermatol Ther 11: 247.

www.doi.org/10.29011/2575-8268.100247

www.gavinpublishers.com

GAVIN PUBLISHERS

Research Article

Sex-Specific Metabolic Remodelling in Infantile Haemangioma

Raka Mitra[1,2], Bridget Chang-McDonald[1], Tracy K Hale[2], Helen L Fitzsimons[2], Clint Gray[1,3*]

[1]Gillies McIndoe Research Institute, Newtown, Wellington 6021, New Zealand.

[2]School of Food Technology and Natural Sciences, Massey University, Palmerston North, New Zealand

[3]Centre for Biodiscovery and School of Biological Sciences, Victoria University of Wellington, Kelburn, Wellington 6021, New Zealand.

***Corresponding Author:** Clint Gray, Director, Gillies McIndoe Research Institute Level 3, 7 Hospital Road, Newtown, Wellington 6021, New Zealand.

Citation: Mitra R, Chang-McDonald B, Hale TK, Fitzsimons HL, Gray C (2026) Sex-Specific Metabolic Remodelling in Infantile Haemangioma. Clin Exp Dermatol Ther 11: 247. DOI: https://doi.org/10.29011/2575-8268.100247

Received Date: 12 February, 2026; **Accepted Date:** 12 March, 2026; **Published Date:** 16 March, 2026

Abstract

Infantile Haemangioma (IH) is the most frequent vascular tumour in infants, characterised by aberrant angiogenesis in the first year of life with propranolol (β-blocker) being the primary treatment option, although the pathogenesis is poorly understood. We performed proteomic profiling of IH patient samples across its three phases– proliferating, plateau and involuting in males and females, and healthy skin controls, with validation by western blot and PCR array. Bioinformatics revealed differential expression in LXR/RXR activation, DHCR24 signalling, and mitochondrial dysfunction. Oxidative phosphorylation complexes I and IV were highly expressed in female proliferating IH, with increased oxidative stress. Further, we validated the regulation of cholesterol homeostasis in IH using PCR array. Proliferation, migration and angiogenesis were upregulated in female lesions compared to males, possibly explaining the higher severity and incidence in females. In summary, we have generated the proteomic landscape of IH in both sexes identifying altered pathways and potential therapeutic targets.

Capsule summary

- Infantile Haemangioma is the most common benign vascular tumour in infants, affecting females three times more than males, yet its pathogenesis remains unknown.
- This proteomic study highlights the sex-based variations in the development of Infantile Haemangioma, that can improve clinical outcomes in patients as potential therapeutic targets.

Keywords: Proteomics; Infantile Haemangioma; Vascular Anomalies; Paediatric; Sex-differences; Mitochondrial Dysfunction; Cholesterol Metabolism.

Introduction

Infantile Haemangioma (IH) affects 10-12% of infants and is the most common benign vascular tumour in childhood, characterised by rapid proliferation in the first year of life followed by gradual regression [1-3]. Risk factors include female sex (3:1 female to male ratio), low birth weight, prematurity, Caucasian ethnicity, maternal factors, and a family history of haemangiomas [4-7]. Although IH involutes spontaneously, 10% develop complications such as scarring, ulceration, tissue distortion and functional problems [4,7-11]. The pathogenesis of IH is not fully understood although it has been characterised to involve dysregulated angiogenesis, hypoxia-driven signalling, NOTCH and PI3K/Akt/mTOR signalling pathways [12-14]. During the proliferating phase, endothelial cell differentiation and migration are regulated by pro-angiogenic factors such as VEGFR2, ANGPT2 and HIF-1α, with downstream MEK/ERK, PI3K/Akt/mTOR, PKC signalling further supporting growth [14-22]. This rapid formation of vascular network slows down in the plateau or quiescence phase. Involution is marked by adipogenesis, apoptosis, and lipid deposition, driven by PPARγ/CEBP and IGF-1 pathway, while suppressing endothelial survival and angiogenesis [12,23-25]. Current treatment approaches depend on location and size of the tumour with the risk of complications, and may include surgery, laser therapy, and β-blockers such as propranolol [1,8,9,26-29]. Propranolol has revolutionised IH management due to its ability to stop growth [21,30-34]. However, its long-term effects on vascular and metabolic development remain unclear, with poor response or relapse in females and severe lesions [7,35-39].

Mechanistic studies implicate regulation of SOX-18-mevalonate pathway, glycolysis and fatty acid oxidation [24,40-47]. The pronounced female predominance suggests hormonal modulation in IH development [48-52]. Metabolic profiling of haemangioma endothelial cells revealed elevated amino acid metabolism [54]. Given these hormonal and pathway alterations in IH, a comprehensive understanding of the proteomic landscape will improve our knowledge of its pathogenesis to fully characterise the underlying molecular landscape. Proteomic profiling, including mass-spectrometry-based approaches, will enable identification of proteins and associated post-translational modifications (PTMs), revealing alterations in differential signalling pathways. In this study, we investigate the proteomic changes across the developmental phases of IH in both sexes with healthy skin samples as controls for differential analysis. Significantly altered proteins were mapped and validated using western blot and PCR array. This represents the most extensive proteomic analysis of IH to date, providing insight to phase- and sex-based molecular differences, and associated pathways that may serve as promising therapeutic targets or biomarkers in IH.

Materials and Methods

Patient samples and study design

This case-control study involved proteomic profiling of IH patient tissue samples and healthy skin controls, collected at Centre for the Study & Treatment of Vascular Birthmarks (Lower Hutt, New Zealand) between 2015-2023. Snap-frozen samples were sourced from Gillies McIndoe Research Institute Biobank, New Zealand in accordance with the ethical standards, approved by the Wellington Ethics Committee (Ref.13/CEN/130). All procedures involving human subjects adhered to the principles of respect, confidentiality and ethical guidelines. Clinical and histological details are presented in Supplementary Table 1. IH samples were grouped as proliferating (0-10 months) (n = 12), quiescent or plateau (12-18 months) (n = 8), involuting (18 months-4 years) (n = 8), and normal skin (8-11 years) (n = 8) with equal males and females.

Protein extraction and digestion

Snap-frozen tissue samples were grounded in liquid nitrogen and lysed in 5% Sodium dodecyl sulphate (Sigma-Aldrich) buffer and protease inhibitor (Thermo Fisher). Lysates were homogenised, sonicated and quantified by BCA assay (Pierce BCA protein kit, Thermo Fisher). Protein reduction, alkylation, and on-column tryptic digestion were performed on S-Trap Micro spin column (Protifi) using established protocols [76,77]. Peptides were eluted, dried and reconstituted for analysis.

Quantification of protein and functional pathway analysis

Peptides were analysed by Liquid chromatography tandem mass spectrometry (LC-MS/MS) and searched against an in silico tryptic digest of *Homo sapiens* proteins from the UniProtKB/Swiss-Prot + TrEMBL sequence database (version August 2024). Proteins were detected with 95% probability (Protein False Discovery Rate = 0.1%) in Spectronaut (Biognosys), and label-free quantification (LFQ) performed using normalised peptide intensities. LFQ values were log2 transformed and filtered (≥ 70% valid values) in Perseus (Maxquant) [76]. Missing values were imputed from a normal distribution, and differential expression assessed via unpaired Student's t-test ($p \leq 0.05$; fold change ≥ 1.2). Ingenuity Pathway analysis (IPA) (Qiagen) identified enriched biological networks and predicted activation states (Fisher's exact test, $p \leq 0.05$).

RNA extraction and PCR array

Total RNA was extracted from proliferating IH (n = 8), involuting IH (n = 6) and normal skin (n = 6) samples using RNeasy kits (Qiagen). cDNA was synthesised using the RT2 First Strand kit

(Qiagen) and profiled with the Human Lipoprotein Signalling and Cholesterol Metabolism RT2 Profiler PCR array (Qiagen). Ct values were normalised to housekeeping genes and analysed using ΔΔCt method.

Western blotting

Lysates from proliferating (n = 8) and involuting IH (n = 6) were separated on 8% or 4-12% Bis-Tris gels (Thermo Fisher), transferred to a nitrocellulose or polyvinylidene difluoride membrane (Bio-Rad), and probed with primary antibodies: OXPHOS complexes (#ab110411, Mouse, 1:1000, Abcam), MAOA (#ab126751, Rabbit, 1:1000, Abcam), Na+K+ATPase (#23565, Rabbit, 1:1000, Cell Signalling Technologies), VDAC (#4661, Rabbit, 1:1000, Cell Signalling Technologies), FAS (#3180T, Rabbit, 1:1000, Cell Signalling Technologies), AMPK (#2532, Rabbit, 1:1000, Cell Signalling Technologies), followed by HRP-conjugated secondary antibodies. Bands were visualised using chemiluminescence and quantified using ImageLab/ ImageJ software. Uncropped blots are provided in (Supplementary Figures 1-2).

Data analysis

Statistical analyses were performed with GraphPad Prism and Microsoft Excel. Two-group comparisons employed unpaired Student's t-test or Mann-Whitney tests; multiple group comparisons used one-way ANOVA or Kruskal-Wallis test. Statistical significance was defined as $p \leq 0.05$.

Results

Protein identification

Mass-spectrometry-based proteomic analysis was performed to compare protein expression across the IH samples spanning the proliferating, plateau or quiescent and involuting phases, alongside normal skin controls. Spectral data analysed with Spectronaut identified 7977 proteins, followed by normalisation, log-transformation and imputation in Perseus. 5585 proteins were then analysed using IPA to examine the biological and molecular interactions (Supplementary Figure 3). Principal Component Analysis (PCA) revealed a clear distribution of IH and normal skin samples (Figure 1a). Venn diagram indicated substantial overlap of proteins across IH phases (Figure 1b).

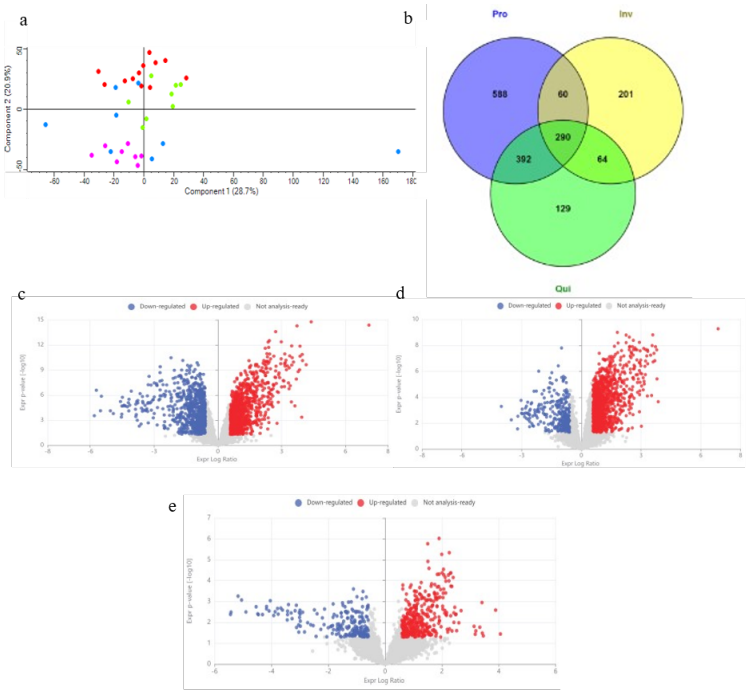

Figure 1: Comparative analysis of the differential protein expression between IH and normal skin; (a) Principal Component Analysis shows clustering of IH samples by clinical phase - proliferating (red), plateau (green) and involuting phase (pink) compared to normal skin (blue); (b) Venn diagram depicting common and unique proteins identified across the three phases of IH. Volcano plot highlights the differential protein expression in proliferating phase; (c), plateau ;(d) and involuting phase ;(e) compared to normal skin. Proteins with a fold change ≥ 1.2 and p-value ≤ 0.05 were considered statistically significant (unpaired student's t-test).

Comparison of protein changes in Infantile Haemangioma and normal skin

Volcano plots showed the distribution of upregulated and downregulated proteins in each phase (Figure 1c-1e). Differential expression analysis used a threshold of fold change ≥ 1.2; p ≤ 0.05. Canonical Pathway Analysis (IPA) identified activated pathways (z scores from -5.831 to 8.310; p ≤ 0.05) (Figure 2). LXR/RXR activation, DHCR24 signalling pathway, xenobiotic metabolism (PXR and AHR), complement cascade and peroxisomal protein import were downregulated in proliferating and plateau phases but not involuting, suggesting early suppression of cholesterol biosynthesis, glutathione-mediated detoxification and activation of gene expression by SREBP. Glucose and triglyceride metabolism were increased in the plateau phase, whereas the apelin adipocyte signalling pathway, matrix metalloproteinase activation, gluconeogenesis and insulin receptor signalling were reduced in proliferating IH (Figure 2).

Figure 2: Heatmap of top significantly expressed canonical pathways under Core Analysis in Ingenuity Pathway Analysis in the phases of IH – proliferating, plateau and involuting, compared to normal skin, p-value ≤ 0.05 (Fisher's exact test).

Sex-specific pathway differences across IH development

Comparative analyses (fold change ≥ 1.2; $p \leq 0.05$) examined molecular differences across sexes (Supplementary Table 2-5). LXR/RXR activation and the DHCR24 signalling pathway were downregulated in female proliferating versus involuting phase (Figure 3a). Key proteins, A1BG, AHSG, ALB, AMBP, APOB, APOC3, APOD, APOH were decreased (Supplementary Table 2), suggesting reduced lipoprotein and cholesterol homeostasis. Collagen biosynthesis and mitochondrial dysfunction were upregulated in the proliferating phase (Supplementary Table 2, Figure 3a), while plateau phase displayed activation of VEGF, RHOA, integrin, and actin cytoskeleton signalling (Figure 3b, Supplementary Table 3), consistent with persistent angiogenesis. Hence, the plateau phase is very similar to proliferating phase in females leading to a slow transition to the involuting phase. Oxidative phosphorylation (OXPHOS) complexes I (NDUFA4L2) and IV (COX4L2, COX7A2L) were selectively upregulated in proliferating female IH while MAOA and Na+K+ATPase decreased (Supplementary Table 2).

LXR/RXR activation and DHCR24 signalling pathway were similarly downregulated in male proliferating and plateau phases versus involuting (Figure 3c-3d, Supplementary Table 4-5). DNA damage/telomere stress induced senescence were activated in male plateau IH demonstrating transition to involution (Figure 3d, Supplementary Table 5). Downstream biological processes indicated higher cell viability, migration, invasion and cellular homeostasis in female lesions compared to males (Figure 3e), suggesting aggressive growth and slow phase transitions in female IH.

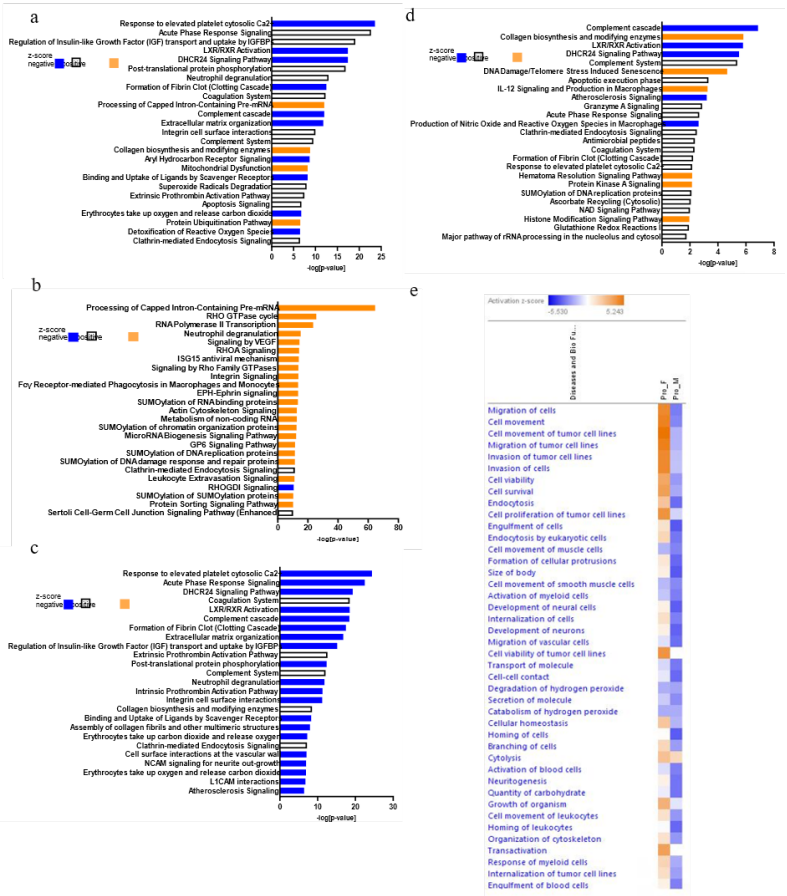

Figure 3: Pathway analyses and functional annotation in IH, using IPA; Bar chart displays the top enriched canonical pathways identified through core analysis in proliferating phase in females; (a), plateau in females; (b), proliferating phase in males; (c), plateau in males; (d) compared to the involuting phase. Pathways are ranked based on -log(p-value) ≥ 1.3 (p-value ≤ 0.05); (e) Heatmap of comparison analysis of downstream biological processes in the female and male proliferating tumours, p-value ≤ 0.05 (Fisher's exact test). Colour coding represents z scores: orange for activation (positive), white for no predicted change (0) and blue for inhibition (negative).

Validation by Western blotting

Proteins involved in mitochondrial dysfunction and lipoprotein signalling - OXPHOS complexes (I-V), MAOA, Na+K+ATPase, VDAC, FAS and AMPK were validated. OXPHOS complexes I and IV were upregulated in the female proliferating phase versus involuting (Figure 4a-4b, Supplementary Table 6); complex II and III reduced in female involuting IH, while complex V elevated in male involuting IH. MAOA expression rose from proliferation to involution (male, $p = 0.004$; female, $p = 0.06$) (Figure 4a-4b). Na+K+ATPase expression was lower in females than males during both phases (proliferating, $p = 0.1$; involuting, $p = 0.04$). AMPK was significantly upregulated in the involuting phase in males compared to females ($p = 0.01$). FAS non-significantly increased in male involuting IH while VDAC was stable (Figure 4b, Supplementary Table 6).

Gene expression of cholesterol metabolism and Lipoprotein signalling

LXR/RXR activation and DHCR24 signalling pathway are key regulators of cholesterol metabolism. 54 genes were differentially expressed in the Human Lipoprotein Signalling and Cholesterol metabolism PCR array in proliferating and involuting phases of IH versus normal skin (Supplementary Table 7), with 19 genes significantly altered (fold-change ≥ 1.5, $p \leq 0.05$) between proliferating and involuting IH (Supplementary Table 8, Figure 4c).

They were further classified as, LDL associated proteins and receptors (*ANKRA2, APOD, CEL, LRP10, LRP1B, STAB2*), cholesterol homoeostasis (*ABCG1, ANGPTL3, HDLBP, INSIG2, LCAT, PPARD, SREBF1)* and cholesterol biosynthesis (*ACAA2, CNBP, IDI2, NSHDL, PRKAA1, PRKAG2)* (Figure 4c). Several sex-specific differences were observed in the proliferating and involuting phases as well, suggesting differential cholesterol regulation across IH development (Figure 4d-4e).

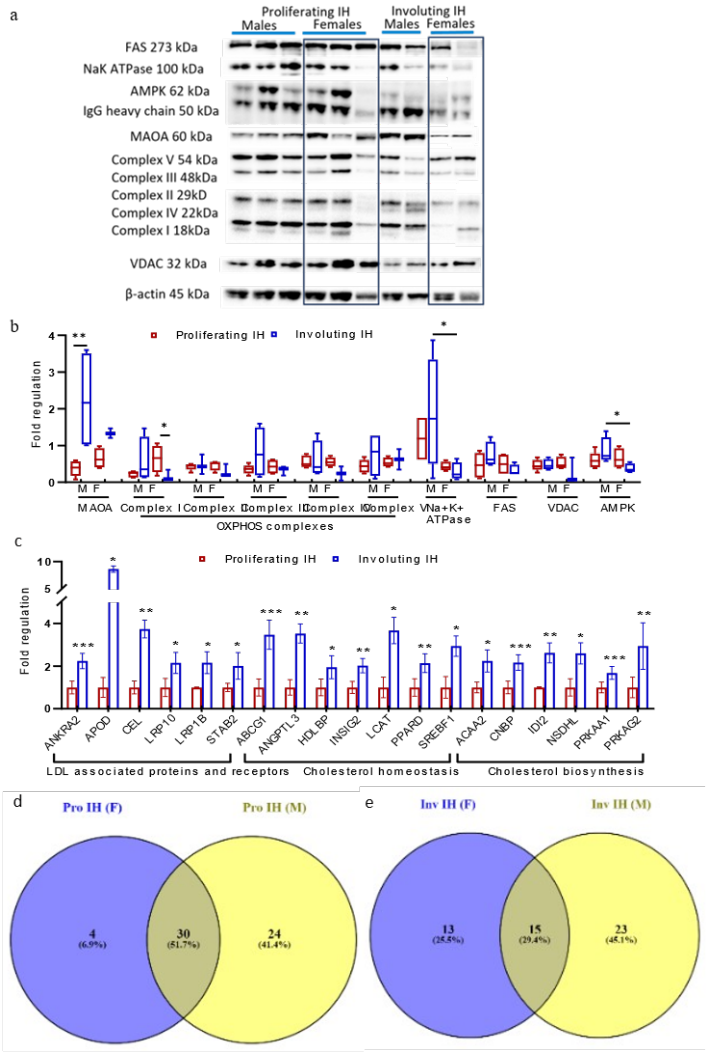

Figure 4: Validation of proteins using Western Blot and gene expression profiling in proliferating and involuting IH; (a) Western Blot analysis of FAS, Na+K+ATPase, AMPK, MAOA, OXPHOS Complexes I-V, VDAC across representative proliferating and involuting phase in female and male patients. β-actin was used as loading control; (b) Box and whisker plot representing Western Blot quantification of MAOA, OXPHOS Complexes I-V, Na+K+ATPase, FAS, VDAC, AMPK normalised to β-actin. Each box represents the interquartile range (Q1, 25th to Q3, 75th percentiles), the central horizontal line is the median value, and the whiskers represent the range. Statistical significance is shown by, *p-value ≤ 0.05, **p-value ≤ 0.01. Proliferating IH, n = 10 (5 male, 5 females), Involuting IH n = 8 (4 male, 4 females); (c) Bar graph shows the fold regulation of genes associated with LDL receptor, cholesterol biosynthesis, and homeostasis in the proliferating and involuting IH. Clinical details of the IH samples

(part of the proteomics dataset) used in this figure are provided in Supplementary Table 1. Venn diagram depicting the variation of gene expression in males and females in proliferating; (d) and involuting phase; (e) Quantitative data plotted as mean ± standard error. Statistical significance is shown by, *p-value ≤ 0.05, **p-value ≤ 0.01, ***p-value ≤ 0.001. Proliferating IH, n = 8 (4 males, 4 females), Involuting IH n = 6 (3 males, 3 females)..

Discussion

In this study, we have performed shotgun proteomics on IH tissue samples from the three phases - proliferating, plateau and involuting compared to normal skin and examined sex-specific differences. Using label-free LC-MS/MS methods, we identified dysregulated proteins and pathways underlying IH pathogenesis. DEPs were analysed across all phases of IH versus normal skin as control, and between proliferating/ plateau and involuting phases in both sexes. Among the top differentially expressed pathways, LXR/RXR activation and DHCR24 signalling pathway increased from proliferating to involuting phase in both sexes. Both are associated with cholesterol metabolism and lipoprotein signalling [54-57], reflecting the regulation of angiogenesis in this highly vascular tumour. SOX18 has previously been implicated in cholesterol metabolism during endothelial differentiation from haemangioma stem cells [40,42,43]. AIBP, a player in cholesterol metabolism negatively correlates with hypoxia-inducible factor 1-alpha (HIF-1α) signalling and inhibits angiogenesis [58].

Cholesterol biosynthesis involves the rate-limiting enzyme HMGCR (3-Hydroxy-3-Methylglutaryl-Coenzyme A Reductase) and DHCR24 (24-Dehydrocholesterol Reductase), regulated transcriptionally and translationally by sterol intermediates [55,56,59]. Proliferating IH showed downregulation of cholesterol homeostasis (*ABCG1, ANGPTL3, HDLBP, INSIG2, LCAT, PPARD, SREBF1, CETP*), and biosynthesis (*ACAA2, CEL, CNBP, IDI2, NDSHL, PRKAA1, PRKAG2*), likely due to intracellular cholesterol accumulation, and feedback regulation [40].

Reduced LDL receptors (*ANKRA2, APOD, CEL, CNBP, LRP10, LRP1B, STAB2*) and LXR/RXR signalling pathway further promote cholesterol buildup due to disrupted degradation and efflux, and consequently a metabolic shift from anabolic toward catabolic pathways (Figure 5) [54,57,60]. Proteomic analyses revealed decreased Insulin-like growth factor (IGF) transport regulation by IGFBPs in proliferating phase, consistent with genome-wide transcriptional profiling in IH [23,62]. IGF-signalling maintains electron transport chain function and mitigates oxidative stress, while IGFBPs stop IGF-activity inducing apoptosis [61-64].

Mitochondrial dysfunction was upregulated during proliferation, particularly OXPHOS complexes I and IV in female IH, suggesting sex-based variation in IH development. Concurrently, glutathione-mediated detoxification may increase oxidative stress, establishing a regulatory relationship of mitochondrial dysfunction, cholesterol metabolism and increased angiogenesis (Figure 5) [60,65]. IH's hypoxic environment drives glycolytic reprogramming via HIF-1α [44,45,66,67]. Increased OXPHOS complex I elevates reactive oxygen species generation, while complex IV maintains ATP generation and protects from oxidative stress enabling endothelial survival [44,47,68-72]. This glycolytic dependence reflects metabolic adaptation during IH proliferation. Sex differences were pronounced with increased proliferation and vasculogenesis in female tumours compared to males. Increased FAS and AMPK in males, reflects enhanced lipid synthesis in the involuting phase. Complications associated with IH, recurrence and poor response to propranolol are also more common in females [35,36], potentially due to increased angiogenesis, mitochondrial dysfunction, and cholesterol metabolism. The influence of sex hormones on sterol homeostasis in IH also warrants further investigation.

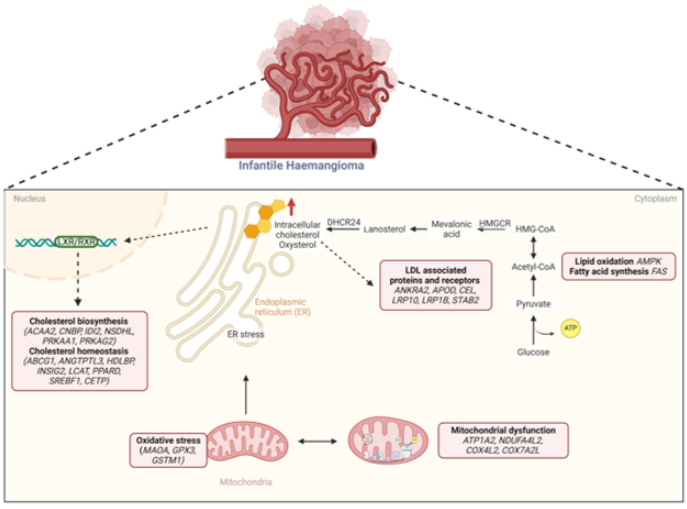

Figure 5: Schematic illustration of the regulatory relationship between cholesterol homeostasis and mitochondrial dysfunction driving the pathogenesis of IH; In the proliferating phase, elevated intracellular cholesterol levels lead to downregulation of HMGCR, the rate limiting enzyme of cholesterol synthesis. Concurrently, reduced LXR/RXR mediated transcription (*ANKRA2, APOD, CEL, LRP10, LRP1B, STAB2*) result in sterol accumulation and increased endoplasmic reticulum stress by regulation of cholesterol homeostasis (*ABCG1, ANGTPTL3, HDLBP, INSIG2, LCAT, PPARD, SREBF1, CETP*)) and biosynthesis (*ACAA2, CNBP, IDI2, NSDHL, PRKAA1, PRKAG2*). Increased mitochondrial dysfunction in the proliferating phase is also associated with cholesterol accumulation by elevated OXPHOS complex I (NDUFA4L2). Elevated expression of complex IV (COX4L2, COX7A2L), decreased MAOA and dysregulated oxidative phosphorylation

contribute to oxidative stress (GPX3, GSTM1). Additionally, lipid oxidation and fatty acid synthesis are also regulated by AMPK and FAS respectively with an increased glycolysis further supporting the synthesis of Acetyl-CoA and hence increased sterol (created in Biorender.com).

Current treatments like propranolol target endothelial glycolysis and accelerating involution [33,34,47,73-75]. R-isomer of propranolol inhibits SOX18 disrupting the mevalonate pathway, essential for cholesterol biosynthesis and endothelial differentiation [40,43] underscoring the therapeutic relevance of these pathways. Functional validation in different IH cell subtypes need to be investigated to elucidate the interplay between mitochondrial dysfunction and cholesterol homeostasis. In summary, our results portray the IH proteome from proliferating, plateau to involuting across sexes, filling an important gap in understanding the molecular mechanisms behind IH pathogenesis. Our proteomic data establish the regulatory relationship between oxidative stress, accumulation of intracellular cholesterol and dysfunctional electron transport chain in mitochondria, particularly under hypoxic conditions, playing key roles in the development and progression of IH.

Acknowledgments

We would like to acknowledge the Hutt Valley Hospital and Centre for the Study & Treatment of Vascular Birthmarks, Lower Hutt, New Zealand, for tissue samples; the patients who provided the tissues and Dr Swee Tan.

Author contributions: Conceptualization: CG, RM, BCM; Methodology: RM, CG; Investigation: RM, CG; Visualization: RM, CG; Funding acquisition: CG; Project administration: CG; Supervision: CG; Writing – original draft: RM, CG; Writing – review & editing: RM, CG, TKH, HLF.

Data and materials availability: Data is contained within the article and the supplementary. The mass spectrometry proteomics data have been deposited to the ProteomeXchange Consortium (http://proteomecentral.proteomexchange.org) via the PRIDE [79] partner repository with the dataset identifier PXD069224.

Funding sources: This study was funded by the Deanes Endowment Trust and H & R Whitehouse Fund.

Conflicts of Interest: None declared.

References

1. Chen ZY, Wang QN, Zhu YH, Zhou LY, Xu T, et al. (2019) Progress in the treatment of infantile hemangioma. Ann Transl Med 7: 692.
2. Eisenstein KA (2023) Infantile Hemangiomas: A Review and Future Opportunities. Mo Med 120: 49-52.
3. Nguyen HL, Boon LM, Vikkula M (2020) Genetics of vascular anomalies. Seminars in Pediatric Surgery 29: 150967.
4. Lee KC, Bercovitch L (2013) Update on infantile hemangiomas. Seminars in Perinatology 37: 49-58.
5. Lin Q, Cai B, Shan X, Ni X, Chen X, et al. (2023) Global research trends of infantile hemangioma: A bibliometric and visualization analysis from 2000 to 2022. Heliyon 9: e21300.
6. Matić A, Matić M (2025) Infantile Hemangiomas in Very and Extremely Preterm Infants: Incidence and Main Characteristics. Clin Exp Dermatol 51: 21-26.
7. Xu W, Zhao H (2022) Management of infantile hemangiomas: Recent advances. Frontiers in Oncology 12: 1064048.
8. Rešić A, Barčot Z, Habek D, Pogorelić Z, Bašković M (2025) The Evaluation, Diagnosis, and Management of Infantile Hemangiomas—A Comprehensive Review. Journal of Clinical Medicine, 14: 425-425.
9. Cheng CE, Friedlander SF (2016) Infantile hemangiomas, complications and treatments. Seminars in Cutaneous Medicine and Surgery 35: 108-116.
10. Baselga E, Roe E, Coulie J, Muz FZ, Boon LM, et al. (2016) Risk Factors for Degree and Type of Sequelae After Involution of Untreated Hemangiomas of Infancy. JAMA Dermatol 152: 1239-1243.
11. Fernández Faith E, Shah SD, Braun M, Pope E, Lara-Corrales I, et al. (2023) Incidence and clinical factors associated with ulceration in infantile hemangiomas. J Am Acad Dermatol 88: 414-420.
12. Chen Q, Zheng J, Bian Q (2024) Cell Fate Regulation During the Development of Infantile Hemangioma. J Invest Dermatol 145: 266-279.
13. Xiang S, Gong X, Qiu T, Zhou J, Yang K, et al. (2024) Insights into the mechanisms of angiogenesis in infantile hemangioma. Biomedicine & Pharmacotherapy 178: 117181.
14. Mitra R, Fitzsimons HL, Hale T, Tan ST, Gray C, et al. (2024) Recent advances in understanding the molecular basis of infantile haemangioma development. Br J Dermatol 191: 661-669.
15. Ji Y, Chen S, Li K, Li L, Xu C, Xiang B (2014) Signaling pathways in the development of infantile hemangioma. J Hematol Oncol 7: 13.
16. Boscolo E, Bischoff J (2009) Vasculogenesis in Infantile Hemangioma. Angiogenesis 12: 197-207.
17. Boye E, Olsen BR (2009) Signaling mechanisms in infantile hemangioma. Curr Opin Hematol 16: 202-208.
18. Greenberger S, Bischoff J (2013) Pathogenesis of infantile haemangioma. Br J Dermatol 169: 12-19.
19. Itinteang T, Withers AHJ, Davis PF, Tan ST (2014) Biology of Infantile Hemangioma. Front Surg 1: 38.
20. Yin RR, Hao D, Chen P (2018) Expression and correlation of MMP-9, VEGF, and p16 in infantile hemangioma. Eur Rev Med Pharmacol Sci 22: 4806-4811.
21. Sun B, Dong C, Lei H, Gong Y, Li M, et al. (2020) Propranolol inhibits proliferation and induces apoptosis of hemangioma-derived endothelial cells via Akt pathway by down-regulating Ang-2 expression. hem Biol Interact 316: 108925.
22. Wang Y, Chen J, Tang W, Zhang Y, Li X (2017) Rapamycin inhibits the proliferation of endothelial cells in hemangioma by blocking the mTOR-FABP4 pathway. Biomed Pharmacother 85: 272-279.

23. Wang F, Li H, Lou Y, Xie J, Cao D, et al. (2019) Insulin-like growth factor I promotes adipogenesis in hemangioma stem cells from infantile hemangiomas. Mol Med Rep 19: 2825-2830.

24. Yuan SM, Guo Y, Wang Q, Xu Y, Wang M, et al. (2017) Over-expression of PPAR-γ2 gene enhances the adipogenic differentiation of hemangioma-derived mesenchymal stem cells *in vitro* and *in vivo*. Oncotarget 8: 115817-115828.

25. Xu X, Wu Y, Li H, Xie J, Cao D, et al. (2021) Notch pathway inhibitor DAPT accelerates *in vitro* proliferation and adipogenesis in infantile hemangioma stem cells. Oncol Lett 22: 854.

26. Satterfield KR, Chambers CB (2019) Current treatment and management of infantile hemangiomas. Surv Ophthalmol 64: 608-618.

27. Soliman YS, Khachemoune A (2018) Infantile hemangiomas: Our current understanding and treatment options. Dermatol Online J 24: 13030.

28. Kowalska M, Dębek W, Matuszczak E (2021) Infantile Hemangiomas: An Update on Pathogenesis and Treatment. J Clin Med 10: 4631.

29. Dahan E, Jaoude LA (2023) Infantile Hemangiomas: A Review of Current Treatment Options. Pediatr Ann 52: 192-197.

30. Tan X, Guo S, Wang C (2021) Propranolol in the Treatment of Infantile Hemangiomas. Clinical, Cosmetic and Investigational Dermatology 14: 1155-1163.

31. Itinteang T, Brasch HD, Tan ST, Day DJ (2011) Expression of components of the renin-angiotensin system in proliferating infantile haemangioma may account for the propranolol-induced accelerated involution. J Plast Reconstr Aesthet Surg 64: 759-765.

32. Léauté-Labrèze C, De La Roque ED, Hubiche T, Boralevi F, Thambo JB, et al. (2008) Propranolol for Severe Hemangiomas of Infancy N Engl J Med 358: 2649-2651.

33. Li HH, Lou Y, Zhang RR, Xie J, Cao DS (2019) Propranolol Accelerats Hemangioma Stem Cell Transformation into Adipocyte. Ann Plast Surg 83: 5-13.

34. Zhu T, Wang P, Wang R, Tong G, Sun Y, et al. (2025) Propranolol accelerates adipogenesis and inhibits endothelium differentiation of HemSCs via suppressing HK2 mediated glycolysis. Pediatr Res 1-11.

35. Hali F, Moubine I, Berrami H, Serhier Z, Othmani MB, et al. (2023) Predictors of poor response to oral propranolol in infantile hemangiomas. Arch Pediatr 30: 455-457.

36. Frongia G, Byeon JO, Mehrabi A, Günther P (2021) Recurrence rate of infantile hemangioma after oral propranolol therapy. Eur J Pediatr 180: 585-590.

37. Yamaguchi Y, Horino S, Miyabayashi H, Aki H, Miura K (2025) New onset bronchial asthma following oral propranolol for infantile hemangioma. Respir Med Case Rep 54: 102187.

38. Wang C, Wang Q, Xiang B, Chen S, Xiong F, et al. (2018) Effects of Propranolol on Neurodevelopmental Outcomes in Patients with Infantile Hemangioma: A Case-Control Study. Biomed Res Int 25: 5821369.

39. Dai Y, Qiu M, Zhang S, Peng J, Hou X, et al. (2023) The Mechanism of Oxymatrine Targeting miR-27a-3p/PPAR-γ Signaling Pathway through m6A Modification to Regulate the Influence on Hemangioma Stem Cells on Propranolol Resistance. Cancers 15: 5213.

40. Holm A, Graus MS, Wylie-Sears J, Borgelt L, Tan JWH, et al. (2024) An endothelial SOX18-mevalonate pathway axis enables repurposing of statins for infantile hemangioma. bioRxiv 29: 577829.

41. Sasaki M, North PE, Elsey J, Bubley J, Rao S, et al. (2019) Propranolol exhibits activity against hemangiomas independent of beta blockade. NPJ Precis Oncol 3: 27.

42. Overman J, Fontaine F, Wylie-Sears J, Moustaqil M, Huang L, et al. (2019) R-propranolol is a small molecule inhibitor of the SOX18 transcription factor in a rare vascular syndrome and hemangioma. Elife 8: e43026.

43. Seebauer CT, Graus MS, Lan Huang, McCann A, Wylie-Sears J, et al. (2022) Non–beta blocker enantiomers of propranolol and atenolol inhibit vasculogenesis in infantile hemangioma. The Journal of Clinical Investigation 132: e151109.

44. Chen J, Wu D, Dong Z, Chen A, Liu S (2020) The expression and role of glycolysis-associated molecules in infantile hemangioma. Life Sci 259: 118215.

45. Wang Y, Kong L, Sun B, Cui J, Shen W (2022) Celecoxib induces adipogenic differentiation of hemangioma-derived mesenchymal stem cells through the PPAR-γ pathway *in vitro* and *in vivo*. Exp Ther Med 23: 375.

46. Yang K, Qiu T, Zhou J, Gong X, Zhang X, et al. (2023) Blockage of glycolysis by targeting PFKFB3 suppresses the development of infantile hemangioma. J Transl Med 21: 85.

47. Yang K, Li X, Qiu T, Zhou J, Gong X, et al. (2023) Effects of propranolol on glucose metabolism in hemangioma-derived endothelial cells. Biochem Pharmacol 218: 115922.

48. Hou F, Dai Y, Fan CY, Suen JY, Richter GT (2018) Estrogen is involved in hemangioma regression associated with mast cells. Orphanet J Rare Dis 13: 181.

49. Maclellan RA, Konczyk DJ, Goss JA, Greene AK (2018) Analysis of Follicle-Stimulating Hormone Receptor in Infantile Hemangioma. Ann Plast Surg 80 :211-213.

50. Johnson A, Zhang H, Gonzalez SR, Lee M, Wei T, et al. (2021) Presence of estrogen and progesterone receptors in proliferating and involuting infantile hemangiomas. J Plast Reconstr Aesthet Surg 74: 3061-3065.

51. Xiao X, Liu J, Sheng M (2004) Synergistic effect of estrogen and VEGF on the proliferation of hemangioma vascular endothelial cells. J Pediatr Surg 39: 1107-1110.

52. Zhang L, Wu HW, Yuan W, Zheng JW (2017) Estrogen-mediated hemangioma-derived stem cells through estrogen receptor-α for infantile hemangioma. Cancer Manag Res :9: 279-286.

53. Yang K, Qiu T, Gong X, Zhou J, Lan Y, et al. (2023) Integrated nontargeted and targeted metabolomics analyses amino acids metabolism in infantile hemangioma. Front Oncol 13: 1132344.

54. Endo-Umeda K, Makishima M (2025) Exploring the Roles of Liver X Receptors in Lipid Metabolism and Immunity in Atherosclerosis. Biomolecules 15: 579.

55. Körner A, Zhou E, Müller C, Mohammed Y, Herceg S, et al. (2019) Inhibition of Δ24-dehydrocholesterol reductase activates pro-resolving lipid mediator biosynthesis and inflammation resolution. Proc Natl Acad Sci U S A 116: 20623-20634.

56. Luu W, Zerenturk EJ, Kristiana I, Bucknal MP, Sharpe LJ, et al. (2014) Signaling regulates activity of DHCR24, the final enzyme in cholesterol synthesis. J Lipid Res 55: 410-420.

57. Wang B, Tontonoz P (2018) Liver X receptors in lipid signalling and membrane homeostasis. Nature Reviews Endocrinology 14: 452-463.

58. Jiang Y, Li X, Liu Q, Lei G, Wu C, et al. (2024) Apolipoprotein A-I Binding Protein Inhibits the Formation of Infantile Hemangioma through Cholesterol-Regulated Hypoxia-Inducible Factor 1α Activation. J Invest Dermatol 144: 645-658.

59. Hashemi M, Hoshyar R, Ande SR, Chen QM, Solomon C, et al. (2016) Mevalonate Cascade and its Regulation in Cholesterol Metabolism in Different Tissues in Health and Disease. Curr Mol Pharmacol 10: 13-26.

60. Bovenga F, Sabbà C, Moschetta A (2015) Uncoupling nuclear receptor LXR and cholesterol metabolism in cancer. Cell Metab 21: 517-526.

61. Calicchio ML, Collins T, Kozakewich HP (2009) Identification of Signaling Systems in Proliferating and Involuting Phase Infantile Hemangiomas by Genome-Wide Transcriptional Profiling. Am J Pathol 174: 1638-1649.

62. Ritter MR, Dorrell MI, Edmonds J, Friedlander SF, Friedlander M (2002) Insulin-like growth factor 2 and potential regulators of hemangioma growth and involution identified by large-scale expression analysis. Proc Natl Acad Sci U S A 99: 7455-7460.

63. Logan S, Pharaoh GA, Marlin MC, Masser DR, Matsuzaki S, et al. (2018) Insulin-like growth factor receptor signaling regulates working memory, mitochondrial metabolism, and amyloid-β uptake in astrocytes. Mol Metab 9: 141-155.

64. Unterluggauer H, Hütter E, Viertler HP, Jansen-Dürr P (2008) Insulin-like growth factor-induced signals activate mitochondrial respiration. Biotechnol J 3: 813-816.

65. Wall CTJ, Lefebvre G, Metairon S, Descombes P, Wiederkehr A, et al. (2022) Mitochondrial respiratory chain dysfunction alters ER sterol sensing and mevalonate pathway activity. J Biol Chem 298: 101652.

66. de Jong S, Itinteang T, Withers AHJ, Davis PF, Tan ST (2016) Does hypoxia play a role in infantile hemangioma? Arch Dermatol Res 308: 219-227.

67. Li M, Wang X, Yang E, Li Y, Geng Y, et al. (2023) OTUB1 Catalytic-Independently Deubiquitinates TGFBI and Mediates the Angiogenesis in Infantile Hemangioma by Regulating Glycolysis. Arterioscler Thromb Vasc Biol 43: 654-673.

68. Goda N, Kanai M (2012) Hypoxia-inducible factors and their roles in energy metabolism. Int J Hematol 95: 457-463.

69. Fuhrmann DC, Brüne B (2017) Mitochondrial composition and function under the control of hypoxia. Redox Biol 12: 208-215.

70. Hsu CC, Tseng LM, Lee HC (2016) Role of mitochondrial dysfunction in cancer progression. Exp Biol Med 241: 1281-1295.

71. Okoye CN, Koren SA, Wojtovich AP (2023) Mitochondrial complex I ROS production and redox signaling in hypoxia. Redox Biol 67: 102926.

72. Kim SH, Singh SV (2022) The FoxQ1 transcription factor is a novel regulator of electron transport chain complex I subunits in human breast cancer cells. Mol Carcinog 61: 372-381.

73. Pan W, Li P, Guo Z, Huang Q, Gao Y (2015) Propranolol induces regression of hemangioma cells via the down□regulation of the PI3K/Akt/eNOS/VEGF pathway. Pediatr Blood Cancer 62: 1414-1420.

74. Tu JB, Ma RZ, Dong Q, Jiang F, Hu XY, Li QY, et al. (2013) Induction of apoptosis in infantile hemangioma endothelial cells by propranolol. Exp Ther Med 6: 574-578.

75. Ji Y, Li K, Xiao X, Zheng S, Xu T, et al. (2012) Effects of propranolol on the proliferation and apoptosis of hemangioma-derived endothelial cells. J Pediatr Surg 47: 2216-2223.

76. Wang F, Veth T, Kuipers M, Altelaar M, Stecker KE (2023) Optimized Suspension Trapping Method for Phosphoproteomics Sample Preparation. Anal Chem 95: 9471-9479.

77. HaileMariam M, Eguez RV, Singh H, Bekele S, Ameni G, et al. (2018) S-Trap, an Ultrafast Sample-Preparation Approach for Shotgun Proteomics. J Proteome Res 17: 2917-2924.

78. Rudolph JD, Cox J (2019) A Network Module for the Perseus Software for Computational Proteomics Facilitates Proteome Interaction Graph Analysis. J Proteome Res 18: 2052-2064.

79. Perez-Riverol Y, Bandla C, Kundu DJ, Kamatchinathan S, Bai J, et al. (2025) The PRIDE database at 20 years: 2025 update. Nucleic Acids Res 53: 543-553.